Contents lists available at ScienceDirect

International Journal of Pharmaceutics: X

End-point determination of heterogeneous formulations using inline torque measurements for a high-shear wet granulation process

Ashley Dan [a], Haresh Vaswani [a], Alice Šimonová [b,c], Aleksandra Grząbka-Zasadzińska [d], Jingzhe Li [e], Koyel Sen [e], Shubhajit Paul [e], Yin-Chao Tseng [e], Rohit Ramachandran [a,*]

[a] Department of Chemical and Biochemical Engineering, Rutgers, The State University of New Jersey, Piscataway, NJ, USA 08854
[b] Department of Analytical Chemistry, Charles University, Hlavova 2030/8, 12843, Prague, Czech Republic
[c] Zentiva k. s., U Kabelovny 130, Prague, Czech Republic
[d] Institute of Chemical Technology and Engineering, Poznan University of Technology, ul. Berdychowo 4, 60-965 Poznań, Poland
[e] Boehringer Ingelheim Pharmaceuticals Inc, 900 Ridgebury Rd, Ridgefield, CT 06877, United States of America

ARTICLE INFO

ABSTRACT

In this study, the torque profiles of heterogeneous granulation formulations with varying powder properties in terms of particle size, solubility, deformability, and wettability, were studied, and the feasibility of identifying the end-point of the granulation process for each formulation based on the torque profiles was evaluated. Dynamic median particle size (d_{50}) and porosity were correlated to the torque measurements to understand the relationship between torque and granule properties, and to validate distinction between different granulation stages based on the torque profiles made in previous studies. Generally, the torque curves obtained from the different granulation runs in this experimental design could be categorized into two different types of torque profiles. The primary factor influencing the likelihood of producing each profile was the binder type used in the formulation. A lower viscosity, higher solubility binder resulted in a type 1 profile. Other contributing factors that affected the torque profiles include API type and impeller speed. Material properties such as the deformability and solubility of the blend formulation and the binder were identified as important factors affecting both granule growth and the type of torque profiles observed. By correlating dynamic granule properties with torque values, it was possible to determine the granulation end-point based on a pre-determined target median particle size (d_{50}) range which corresponded to specific markers identified in the torque profiles. In type 1 torque profiles, the end-point markers corresponded to the plateau phase, whereas in type 2 torque profiles the markers were indicated by the inflection point where the slope gradient changes. Additionally, we proposed an alternative method of identification by using the first derivative of the torque values, which facilitates an easier identification of the system approaching the end-point. Overall, this study identified the effects of different variations in formulation parameters on torque profiles and granule properties and implemented an improved method of identification of granulation end-point that is not dependent on the different types of torque profiles observed.

1. Introduction

The Quality-by-Design (QbD) approach, which is endorsed by regulatory agencies such as the U.S. Food and Drug Administration (FDA) and widely implemented in the pharmaceutical industry, has been at the forefront of pharmaceutical research and development. This is due to the benefits that these improvement strategies have brought to product quality and manufacturing productivity (Schweitzer et al. 2010). The key concepts of pharmaceutical QbD begin with a pre-determined

objective, such as target product quality specifications, along with the utilization of product and process understanding to identify and link critical material attributes (CMAs) and critical process parameters (CPPs) to critical quality attributes (CQAs), and finally the use of control strategies to ensure that the targeted specifications are met (Food and Administration, 2009; Yu and Kopcha, 2017). To demonstrate process understanding, it is necessary to define acceptable ranges for critical process parameters (CPPs) of unit operations through product and process design spaces necessary to manufacture formulations with

---

* Corresponding author.
E-mail address: rohitrr@soe.rutgers.edu (R. Ramachandran).

Table 1

API primary powder properties.

API Material	Acetaminophen	Ibuprofen Sodium
d_{10} (μm)	5	51
d_{50} (μm)	42	127
d_{90} (μm)	198	220
Contact Angle (°)	53.35	71.33
Compressibility (at 15 kPa)	66.13	24.46
Solubility in water	Slightly soluble[a]	Soluble[b]

[a] Nagai and Prakongpan 1984
[b] Censi et al. 2013

varying material attributes (Yu et al. 2014). While this process can prove to be tedious, especially for multi-component formulations, due to the various combinations of different materials and process parameters required to be tested, there are techniques available to simplify this process, such as Design of Experiments (DoE) and Process Analytical Technology (PAT). DoEs can be used to determine the CPPs important to each CQAs and to define process design spaces using statistical optimization. PAT, on the other hand, provides real-time monitoring and control of processes or product quality, which can be used online or inline during processes to demonstrate that it is maintained within the design space (Yu et al., 2014; Food and Administration, 2004). The use of PAT is useful in increasing process understanding, reducing time and cost for process development, and introducing better quality control (Simon et al. 2015).

Wet granulation is a process that is ubiquitous in the manufacturing of solid dosage forms, such as tablets and capsules. It involves the agglomeration of fine powders into larger granules by spraying liquid binders onto particles as they are agitated, resulting in an increase in particle size (Iveson, Litster, et al. 2001). Wet granulation is a popular option compared to other solid processing technologies, particularly for multi-component formulations, due to its ability to improve flowability and ensure drug content uniformity in the final drug form (Thapa et al. 2019). However, designing a wet granulation process is often tedious due to complex granulation mechanisms that are a function of equipment, formulation, and process conditions (Liu et al. 2021). These factors can have a significant impact on the intermediate quality attributes attained post-granulation, such as particle size distribution (PSD), content uniformity, and granule porosity (Meng et al. 2016). In turn, these attributes can affect the CQAs of the final drug form, including tablet hardness and dissolution properties.

Since as early as the 1980s, before PAT had even been developed,

studies have investigated power consumption or torque as a tool for monitoring the granulation process (Bier 1979; Leuenberger et al. 1981; Hansuld and Briens 2014). In these early studies, the power consumption profile was used to indicate different phases of the granulation stages and the maximum value reached was identified as the granulation end-point, which describes the point at which sufficient amount of binder has been added to the wet mass, beyond which materials may start to be "over-wetted" (Leuenberger et al. 2009). The power consumption profiles are distinguished into five stages, including the wetting phase, formation of liquid bridges (pendular state), filling up of intergranular voids (funicular state), formation of large clusters (capillary state) and formation of suspensions (Leuenberger et al. 2009; Lin et al. 2019). In the terms of modern granulation rate mechanisms and growth regimes, stage I can be associated with wetting, stages II and III with nucleation and growth, stage IV with rapid growth and finally stage V with over-wetting (Iveson et al., 2001a,b).

Despite the promising results of these early studies, the implementation of power consumption as a PAT monitoring tool has yet to be realized due to interference during the granulation process and complications in associating the measurements to formulation properties. For example, Mackaplow et al. (2000) reported frequent wall build-up and collapse of the materials that affected the torque measurements in

Table 2

DOE factors and levels.

Variable	Factors	Factor Levels	
		Low (−1)	High (+1)
X1	Drug Load (%)	5	30
X2	Impeller Speed (RPM)	275	650
X3	API Type	ACM	IBN
X4	Filler Type	MN	LAC
X5	Binder Type	KVA	HPC-L

Table 3

Run details of the three selected runs from the DOE.

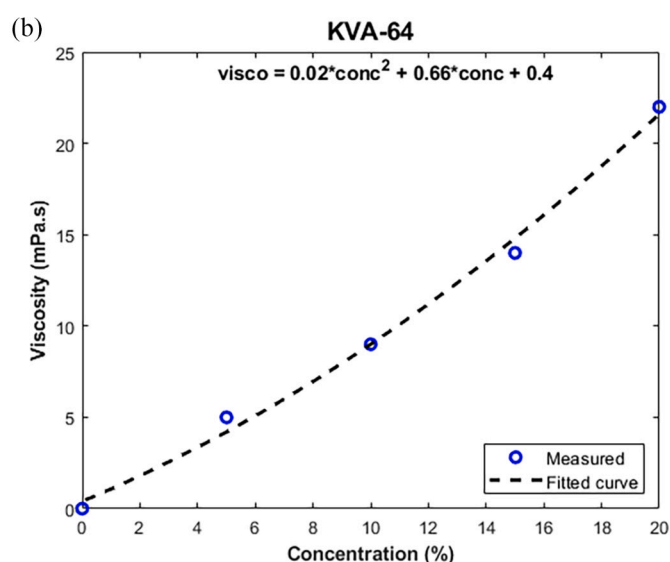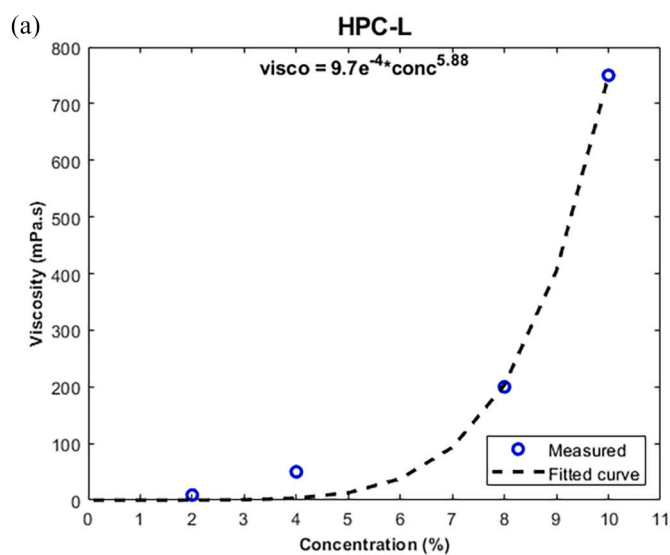| ID	Run Order	Drug Load (%)	Impeller Speed (RPM)	Binder Type	Filler Type	API Type
A	9	20.50	548.75	HPC	MN	ACM
B	10	30	650	KVA	LAC	IBN
C	13	30	650	HPC	LAC	ACM

Fig. 1. Relationship between concentration and viscosity of the two binders used in this study.
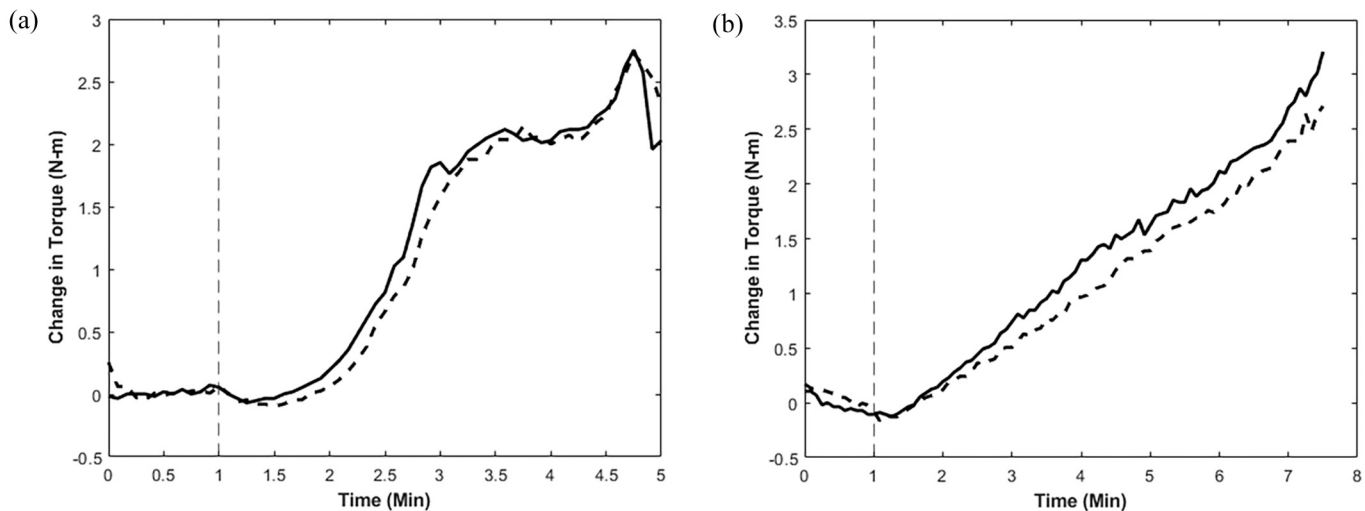
Fig. 2. Torque profiles of (−) initial run and (−-) repeated run with no stops, where the granulation formulation and conditions are (a) Run B, and (b) Run C.
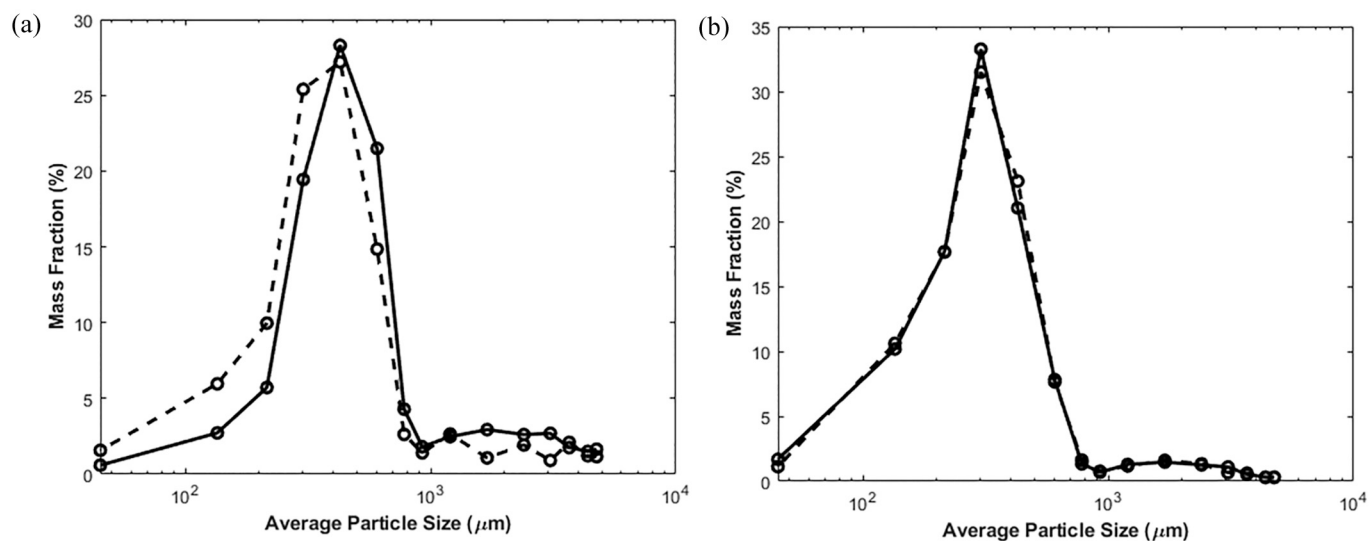

Fig. 3. PSD comparisons between (−) initial run and (−-) repeated run with no stops, where the granulation formulation and conditions are (a) Run B, and (b) Run C.
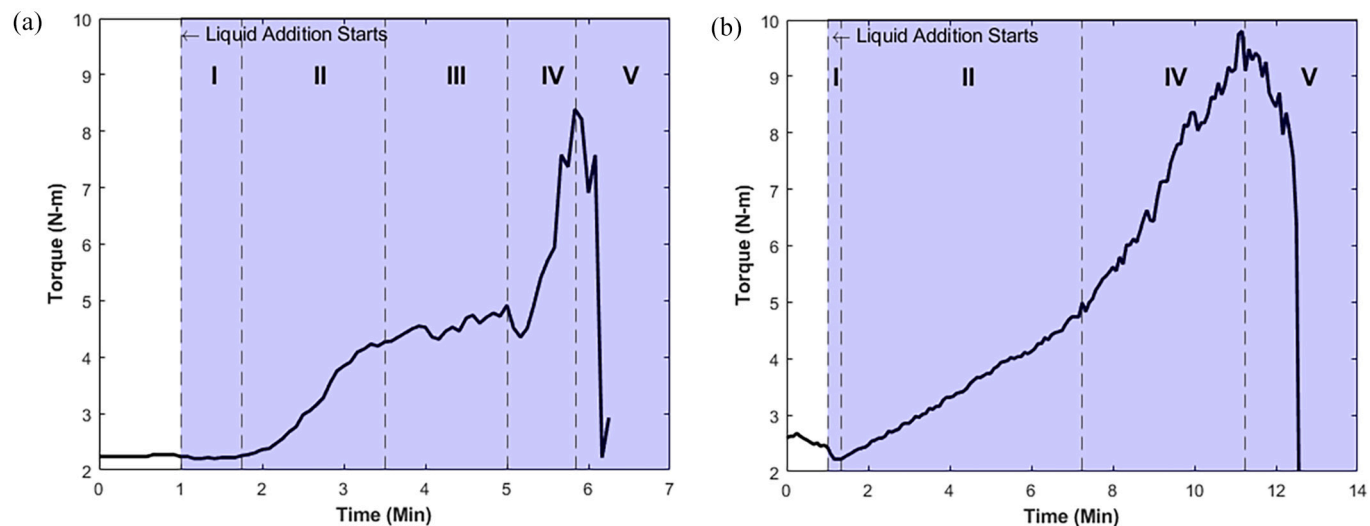

Fig. 4. Different types of torque profiles observed (a) type 1 (from Run B), and (b) type 2 (from Run C).
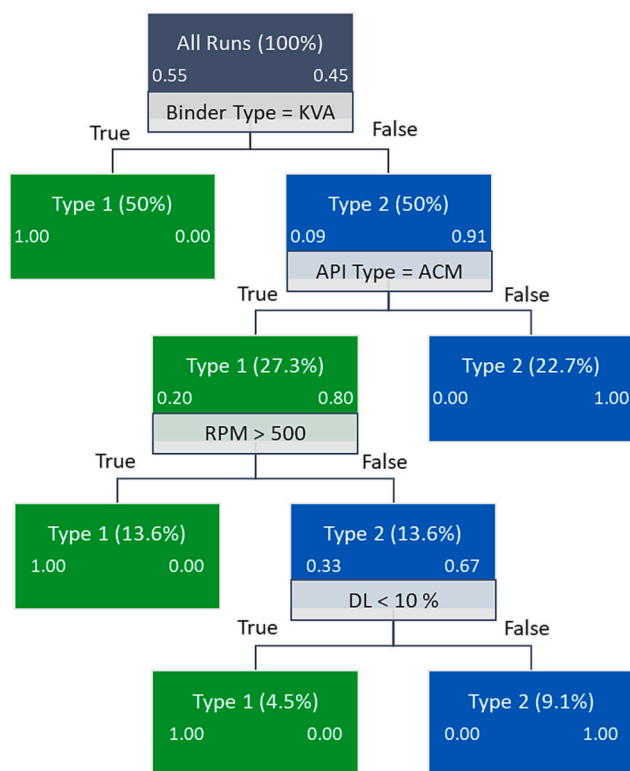
Fig. 5. Classification tree indicating influences of different parameters on the type of torque profile observed (RPM – impeller speed, DL – drug load).

the granulation process. Recent work on the evaluation of torque to control PSD in a continuous twin-screw granulator (TSG) indicated more obstacles, as the torque values indicated not only the energy supplied to rotate the screws but also the energy absorbed by materials (Ryckaert et al. 2021). In the case of the TSG, although torque measurements have been used to capture the energy expenditure during granulation, it is difficult to interpret torque profiles in a manner that provides a good correlation to granulation mechanisms (Sampat et al. 2022). These issues are largely dependent on the scale and the type of equipment used for granulation. Thus, this work will evaluate the feasibility of using torque as a measurement to monitor the granulation process on a KG-5 high shear granulator.

Additionally, there is some ambiguity surrounding the interpretation of the power consumption profiles, as the profiles described by Leuenberger et al. (2009) were only obtained when materials are not too soluble in the granulating liquid, and the binder viscosity is not too high (Leuenberger et al. 2009). In Holm et al.'s (Holm et al. 1985b, 1985a) analysis of power consumption profiles produced during the granulation of either lactose or dicalcium phosphate, they reported the formulations which were able to gain plasticity as liquid is added generated profiles similar to ones described in Leuenberger et al. (2009). However, formulations that largely remain brittle during the liquid addition phase took on a different profile, with the slope increasing slightly at the start until an inflection point where the gradient increases as the power consumption increases rapidly. This continues until the wet mass becomes overwetted and the profile finally plateaus (Holm et al. 1985b). Since the study by Holm et al. (Holm et al. 1985b) was implemented on formulations primarily made up of excipients, there is a need to expand this study to understand the influence of formulation variations in an industrially relevant formulation made up of API, excipient, filler and binder materials, on torque profiles. Cavinato et al. quantified variations in formulation parameters on the minimum liquid volume (MLV) required for granule growth to start occurring and correlated them to dimensionless numbers for regime map analyses (Cavinato et al. 2010; Cavinato et al. 2011; Ly et al. 2021). However, they did not explore the potential differences in torque profiles and granulation end-points that would arise as a result of changes in formulation parameters. This study, therefore, aims to address the above-mentioned gaps by investigating torque measurements of granulation runs of formulations with heterogeneity in blend properties, such as particle size, solubility, wettability, deformability, and density.

Furthermore, many studies have associated the granulation end-point to the point at which the maximum of the torque or power consumption measurement (Sakr et al. 2012; Ly et al. 2021; Otsu et al. 2022), with only a few of these studies giving any regards to the granule quality attributes such as particle size distribution or porosity. By using frequency analysis techniques, Terashita et al. (1990) observed that the fluctuations of power consumption were affected by the particle size distributions and granule growth rate. High fluctuations correlated with a d_{50} that was increasing rapidly, whereas infrequent fluctuations were correlated to slow granule growth rate and approaching the end-point. This study expands on the correlation of torque to other granule attributes, including d_{50} and granule porosity.

The specific objectives of this work are to evaluate the feasibility of using torque measurements as a method to reflect granulation mechanisms and to detect end-point for multiple formulations involving
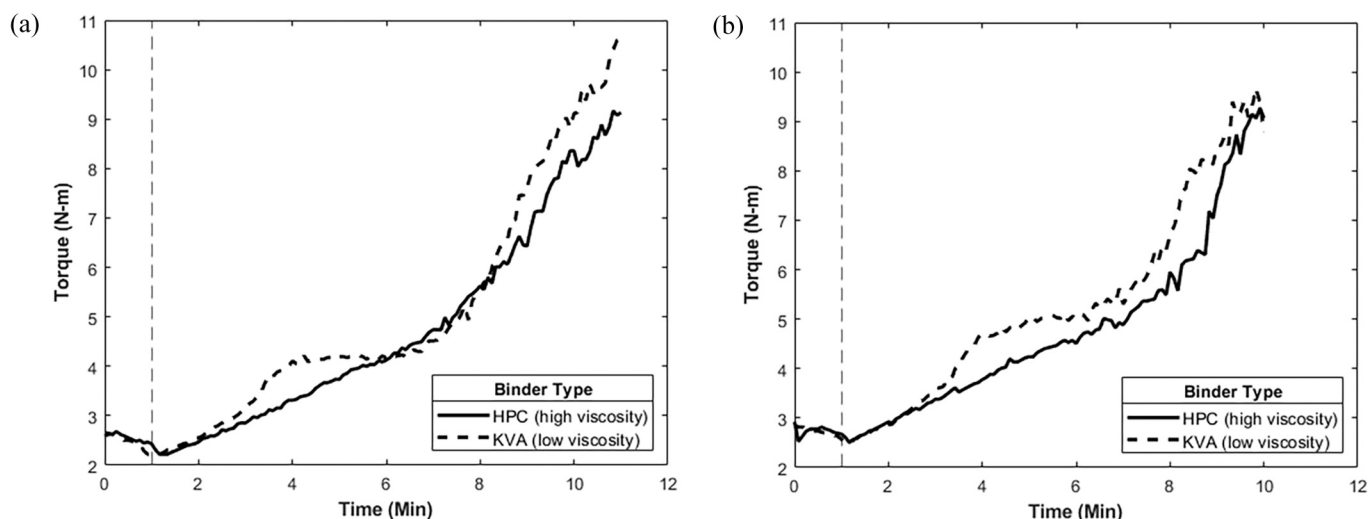

Fig. 6. Effect of binder viscosity on torque measurements for (a) Run A and (b) Run C.
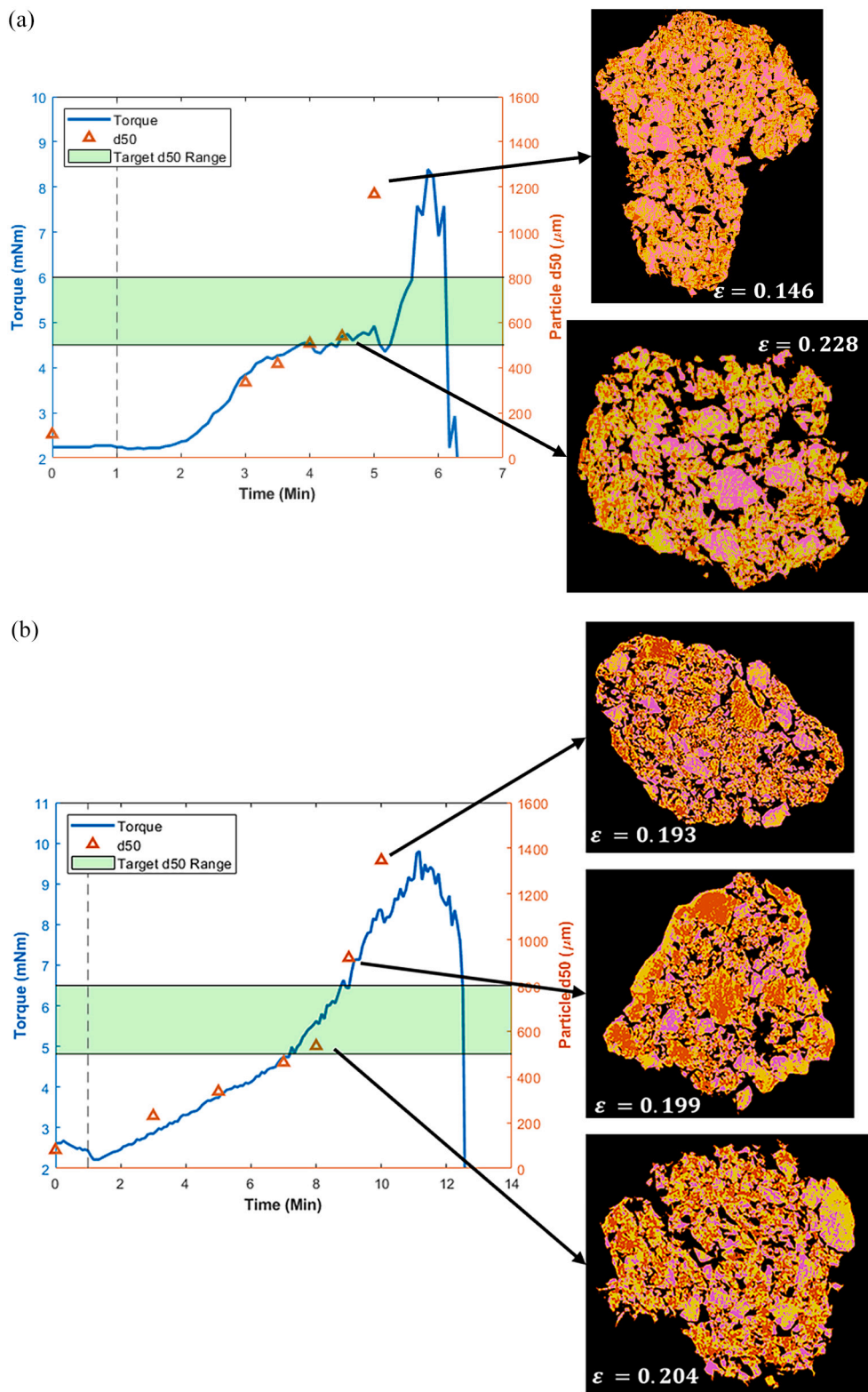
Fig. 7. Relationship between torque, d50, and granule porosity for granulation runs (a) Run B, (b) Run C, and (c) Run A (see details in Table 3).

variations in both formulation and process conditions. Here, the endpoint will be determined based on a target median particle size (d_{50}) range. Hence, the correlation between particle size distribution, porosity and torque measurements will also be determined in this work.

2. Materials and Methods

2.1. Materials

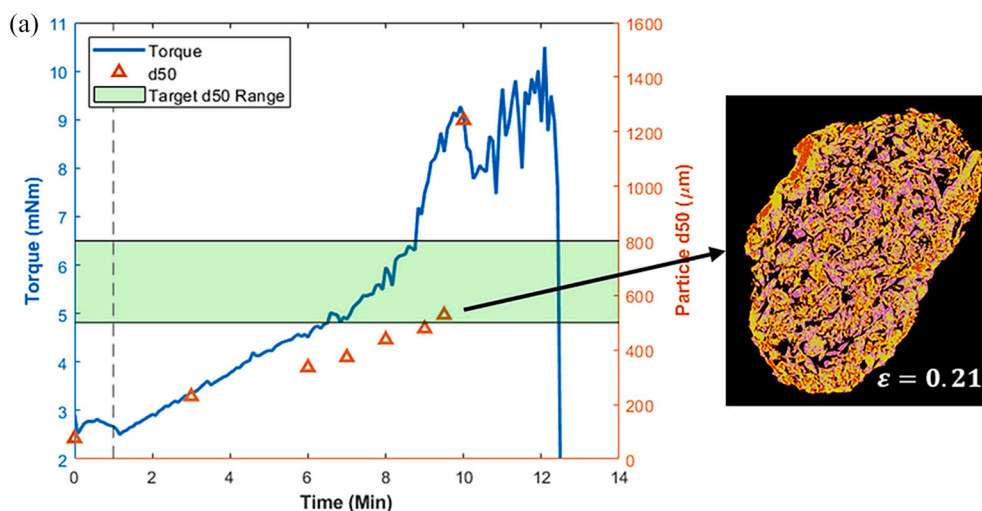In this study, a 5-component industrially relevant formulation was

Fig. 7. (*continued*).

Fig. 8. Paste formed at the end of run B.

used, which includes 1 API, 2 excipients, 1 binder, and 1 disintegrant. The primary properties of the powder were analyzed and presented in Table 1. To incorporate a wide range of heterogeneity in the blend formulations, two different model APIs were selected, one being powder grade Acetaminophen (Spectrum Chemical Mfg. Corp., New Jersey) and Ibuprofen sodium salt (Sigma-Aldrich Inc., Missouri). Each formulation combination contained 2 different excipients - MCC, Avicel 101 grade (Acros Organics, Germany) and either Lactose (BeanTown Chemical, New Hampshire) or Mannitol (MiliporeSigma, Missouri) were used in a 1:2 ratio. A low-viscosity binder,KVA-64 (Kollidon VA64, BASF, Germany) or high-viscosity binder,HPC-L (Hydroxypropyl-cellulose, Nippon Soda Co, Japan) was used. The viscosity-concentration curve for each of the binders are illustrated in Fig. 1. Additionally, a trace amount (1%) of disintegrant,Ac-Di-Sol (Primellose, Dupont Nutrition Ireland, Ireland)was included in the formulation.

2.2. Methods

2.2.1. Equipment details

The granulation experiments were performed in a laboratory scale bench top Key KG5 batch high shear granulator (KEY international Inc., New Jersey), which has a 3.9 L stainless steel bowl, with a top-mounted blade chopper and a 0.203 m impeller. A 400 g batch of pre-blends were blended using a 4-quart V-blender at 20 rpm and tumbled with the use of an intensifier bar for 10 min. The blend was then transferred to the

granulator, and dry mixing was carried out for 1 min before liquid addition started to maintain homogeneity and allow the granulator amps to stabilize. Binders were added to the blend using the dry-binder addition method, where binder powders were incorporated into the powder blend, and deionized water was used as the granulating liquid, which was continuously added at a constant rate of 20 g/min. A 0.1 mm diameter spray nozzle was used to spray the distilled water in the granulator. Once granulation was completed, the granules were dried in a convection oven at 45 °C until the moisture content was below 2% or at a 0.5% difference from the dry pre-blend powders. The moisture content was determined based on the Loss-On-Drying (LOD) method using an MB45 (Ohaus, Corporation, Parsippany, NJ, USA) on a wet basis. Torque measurements were recorded at regular intervals of 5 s from the granulator equipment.2.2.2 Experimental design.

A d-optimal design of experiment (DOE) was formulated using the Design Expert software (Version 13), where six lack-of-fit points and zero replicate points were specified. The five factors used in the DOE design and each respective two parameter levels are listed in Table 2. These five factors include four formulation related parameters and one process parameters, which is impeller speed. In this experimental design, liquid addition time was not specified as an independent factor, instead the granulation process was stopped when liquid addition was deemed completed as usable and robust granules were visibly formed. This formulated DOE based on the d-optimal design contained twenty-two granulation runs. For the purpose of simplification, this study will focus on three selected runs, which will be used in the illustrations in later sections. The three selected runs correspond to the runs requiring the highest, lowest, and median amount of liquid to reach the desired end-point of granulation. The details of these three runs are tabulated in Table 3.

2.2.2. Characterization methods

2.2.2.1. Particle size distribution (PSD).
To determine dynamic particle size distribution, samples were collected intermittently during granulation pauses with the frequency ranging from every 30 s to 2 min based on the rate of granule growth. These samples were collected at the same location in the granulator, which is the furthest away from the liquid addition port to ensure the granules undergo almost a full revolution after coming into contact with the liquid binder. Once air-dried overnight, the volumetric d_{10}, d_{50} and d_{90} of the samples were determined using the Eyecon™ (Innopharma Laboratories, Dublin, Ireland) with their in-built direct image analysis software.
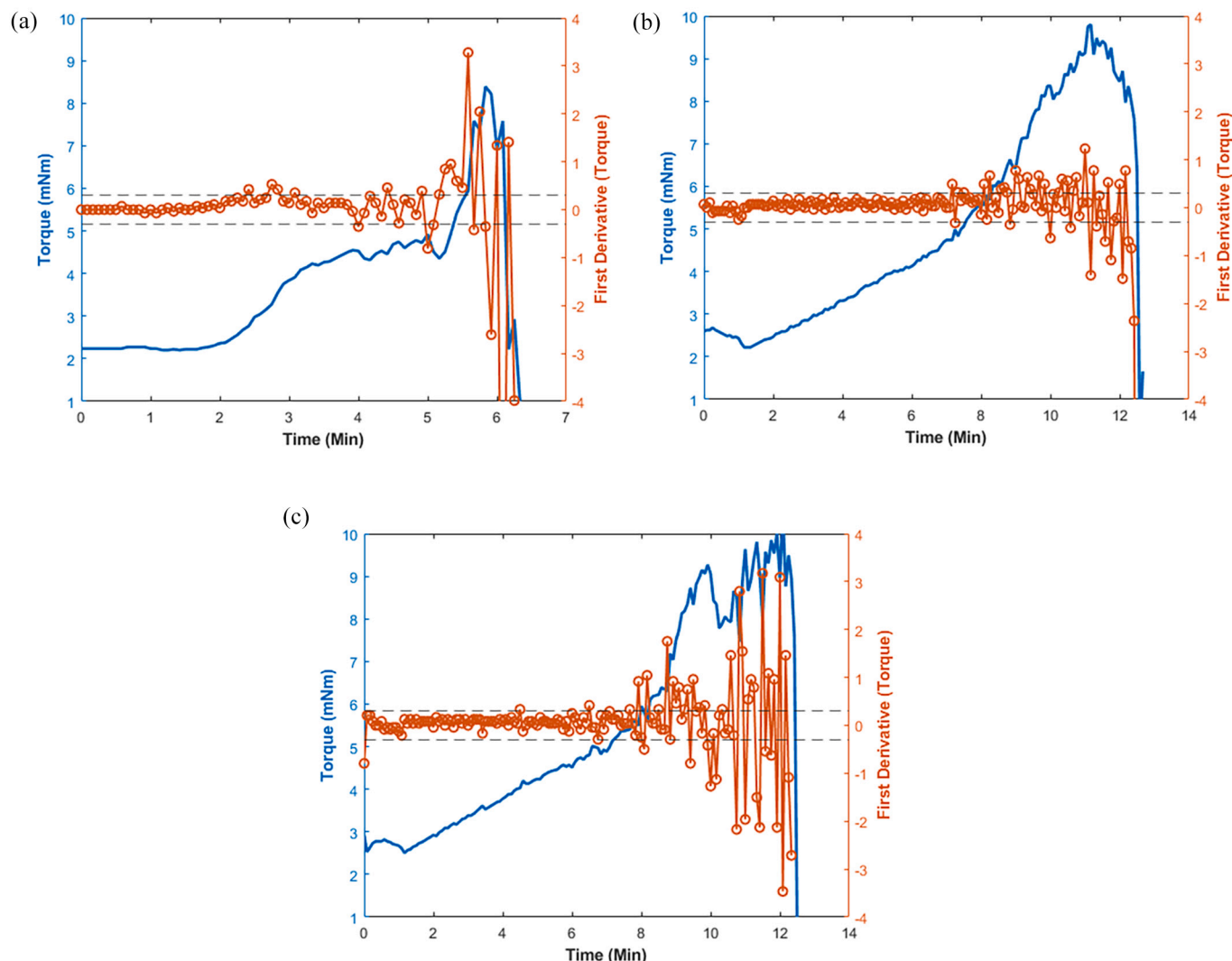
Fig. 9. Torque values (blue) and the first derivative (orange) of the torque values for three different granulation runs, where (a) Run B, (b) Run C, and (c) Run A (see details in Table 3). (For interpretation of the references to colour in this figure legend, the reader is referred to the web version of this article.)

2.2.2.2. Granule porosity. Granule morphology was obtained using scans from micro-computed tomography (micro-CT). The Bruker Sky-Scan 1272 attachment was used to obtain CT scans. A single granule was selected from the 1000–1400 µm sieve and was superglued to a 40 mm untreated plastic micro-hematocrit capillary tube (Safecrit, IRIS International). XY-plane images in slices were reconstructed in the NRecon software (SkyScan). From the reconstructed slices, porosity was determined on the CTAn software (SkyScan), using the Otsu algorithm, which binarizes the images based on the grayscale of pixels. The method of analysis used was based of the protocol developed by Walker et al. in their work of measuring bones with different densities (Walker et al. 2021). A similar analysis of identifying porosity of granules from micro-CT scans was implemented in Kaspar et al. (Kašpar et al. 2013).

2.2.2.3. Contact angle. The sessile drop method was used to measure the contact angle between each component and deionized water. The powder was first compressed into tablet by a flat faced 9 mm diameter punch with 1 s dwell time at a force of 20 kN on a universal testing machine (BlueHill Universal; Instron, Norwood, MA). No surface defects of the tablet were observed. The static contact angle was measured with a drop shape analyzer (Kruss DSA100; Kruss Gmbh, Hamburg, Germany). A syringe needle was positioned approximately 5 mm above from the tablet surface and a drop of deionized water was dispensed.

After dispensing, the drop shape was monitored with a digital camera. The first frame of static liquid drop on tablet surface was used for contact angle calculation. To determine the contact angle, the drop contour was mathematically described by the ellipse method using DSA100, and the contact angle was determined as the slope of the contour line at the three-phase contact point with 3 replicates for each material.

2.2.2.4. Powder compressibility. The Stokes deformation was assessed in terms of compressibility, which was determined for each component on a powder rheometer (FT4; Micromeritics Instrument Corp., Norcross, GA, USA). Initially, the powder was deaerated by downward motion of the impeller for up to 3 cycles to obtain a defined height of the powder column with flat top surface. A ventilated piston was used to apply different normal stress to the powder at 0.5, 1, 2, 4, 6, 8, 10, 12, and 15 kPa, respectively. The compressibility was calculated as the percent volume change at the maximum normal stress with respect to initial condition.

3. Results and Discussion

3.1. Effect of intermittent stops during granulation

Since the granulator had to be stopped periodically for visual

inspection of the granules and sample collection, there were concerns that the changes in bed dynamics that occurred during the stops would affect the granulation mechanisms and granule growth. Hence, two granulation formulations were repeated without stops and the torque and PSDs of the runs were compared. As shown in Fig. 2, the torque profiles for both formulations show a similar trend, but the slopes differ slightly between the runs that operated with and without stops, indicated by the straight and dotted line, respectively. However, the PSD comparison in Fig. 3, shows that the difference was not significant as the PSDs between the runs had good agreement.

3.2. Torque profiles characterization

The interpretation of torque profiles, as developed by Leuenberger et al. (Leuenberger et al. 2009), and studied by many others (Holm et al. 1985b; Bouwman et al. 2005; Lin et al. 2019; Otsu et al. 2022), are often done on torque profiles in the form of.

the type 1 curve, as shown in Fig. 4a, which can be split up into the 5 different stages as described in previous works. However, in our experiments with different formulations, we observed that type 2 curve illustrated in Fig. 4b was a common occurrence. The two curves differ in that type 2 did not appear to go through a stage III plateau phase, instead it transitioned directly from stage II to stage IV. The slope during stage II was also steeper for the type 1 profile. Finally, the duration of stage I, which is the wetting phase, was longer for type 1.

To understand the effect of material properties and process conditions on the profile types, torque profiles from all the runs were quantified and labelled. A simple classification tree was used to categorize different formulation and process conditions to predict the type of torque profiles, with the results shown in Fig. 5. In the first split, we see that all the formulations using KVA, which is the low viscosity binder, produces type 1 profile, whereas both profiles are present for formulations using the high viscosity HPC binder. This occurrence may be attributed to the low viscosity KVA binder having higher solubility in water. While both KVA and HPC are considered water-soluble binders, the study by Köster et al. (2021) indicated that KVA showed a higher hygroscopicity compared to HPC, and a higher hygroscopicity generally correlates to a higher water solubility (Han et al. 2022). Additionally, it was found that the water solubility of KVA was not temperature dependent, whereas HPC is soluble in cold or hot water (Rowe et al. 2009). For formulations with KVA binders, during the wetting stage, the water uptake was able to quickly dissolve the dry binders, and in stage II, which is the nucleation and growth stage, the granules were able to coalesce quickly. This continues until most of the binders have dissolved or the granules have grown to a size that is difficult to coalesce further, at which point stage III begins, where the intergranular voids are being filled. In this stage, granule growth is minimal, resulting in a plateau in the torque values. On the other hand, because of the lower solubility of HPC binders, some formulations had stage II and III occurring simultaneously, resulting in the type 2 curve. To validate these observations, two formulations were repeated with only the binder type altered in the formulation, as displayed in Fig. 6, and the torque profiles in both runs show KVA and HPC represented by the type 1 and type 2 profile, respectively. Here, we see that beginning from Stage IV, the torque profiles observed for both binders start to trend similarly, as both binders are expected to be dissolved by this stage, thus the two runs exhibit similar behavior.

The next split category was the API type and this can be associated with the deformability differences of APIs. Here, we see that the combination of HPC binder and IBN as the API produces the type 2 profile. In comparison, IBN has a higher deformability, as indicated by the lower measured compressibility, shown in Table 1. Materials with lower compressibility require less stress to initiate a permanent deformation, resulting in higher deformability (Paul and Sun 2017). A highly deformable system is more likely to deform due to the impact from collisions, which not only leads to a higher probability of successful coalescence but also results in merged granules having lower porosity

(Iveson and Litster 1998). Consequently, the lower porosity granules with fewer empty voids contribute to the lack of a plateau phase, which was defined as the stage at which particle voids are being filled. Although there was a difference in the primary particle sizes of the APIs, with IBN being larger (Table 1). In theory, the powder particles of IBN and binder droplets are closer in terms of size compared to ACM, thus increasing the likelihood of distributive nucleation mechanisms which is better for coalescence. On the contrary, ACM would be more likely to undergo immersion nucleation, which have more pore saturation (Iveson et al., 2001a). This is in contradiction to the different torque profile types observed. The absence of the effect of API particle sizes could be because this experimental design has drug load varying in the range of 5–30%, so while the two APIs have an obvious size difference, its effect in the blend may not be significant. Impeller speed was used in the following split, where runs with speeds above 500 RPM were observed with the type 1 profile. A low agitation rate can result in both lower granule growth and lower amount of liquid spreading. Under these conditions, it is more likely that stages II and III can happen at the same time. However, impeller speed can sometimes have opposite effects, where at higher impeller speed, the collision frequency is increased, thus resulting in a larger amount of coalescence but can also result in increased occurrence of particle breakage (Oka et al. 2015). This may be the reason for the different torque profile types observed at high impeller speeds.

3.3. Correlation of torque measurements to PSD d_{50} and granule porosity

Particle size, represented by median particle size (d_{50}), showed an increase with increasing torque, which was expected as larger granules have higher frictional resistance (Holm et al. 1985a). The relationship between the torque values and porosity depicted in Fig. 7 was consistent with theories from previous studies that in a type 1 torque profile, particle voids get filled during the plateau phase, as seen in Fig. 7, where the decrease in empty spaces within the granule and lower calculated porosity was apparent. In fact, in both curve types, we observed that the granule porosity decreases as the torque curve approaches the maximum torque value, which is when capillary state is reached, where the interparticle voids are completely filled with liquid (Leuenberger et al. 2009; Belem and Ferraz 2020). However, the decrease in porosity in Fig. 7b was minimal, indicating that in stage IV, pore filling is not prominent. Instead, particles with wetted surface area now coalesce to form larger clusters, indicated by the rapid increase in particle d_{50} in stage IV, which happened for all cases illustrated below. For all three runs, the duration beyond the last available d50 data point signifies the granulation approaching or at the end of stage IV. In stage V, granules start becoming over-wetted and forming clumps of paste, as shown in Fig. 8.

3.4. Determination of granulation end-point

In many granulation experiments, the end goal is to meet desired granule properties that will be beneficial for downstream processing and ensures that the quality attributes of final drug form are within the range target specifications. Some of the common granule attributes that are monitored include PSD and porosity. For this work, the target d_{50} range was between 500 and 800 μm, which are highlighted in green in Fig. 7. The overlayed plots show that if granulation proceeded until the peak torque value was reached, the particle size would be significantly larger and out of range. For the type 1 torque profile, seen in Fig. 7a, the optimum liquid amount to achieve the target size specifications was located at the beginning of the plateau phase. Towards the end of the plateau phase, the d_{50} was noted to increase rapidly. Moreover, the optimum liquid amount for type 2 profile appeared to be in the inflection point of transition between stages II and IV, where a change in the gradient was observed.

While the identification of markers and interpretation of these plots are feasible in hindsight when the entire trend is available, it would be

difficult to identify the end-point while monitoring the torque profiles during the granulation process. Alternatively, perhaps a more helpful perspective of the trend would be the first derivative of the torque values, shown in Fig. 9. This method of analysis was introduced by Cavinato et al. to identify the inflection point between stages I and II to mark the minimum liquid volume required for granule growth to occur (Cavinato et al. 2010). For type 1 torque profiles, denoted in Fig. 9a, we first see a slight increase in the first derivatives during stage II, and later in the second half of the plateau phase, an increase in fluctuations was observed, where the beginning of those fluctuations corresponds to the rapid increase in d_{50}. Similarly, for type 2 profiles, shown in Figs. 9b and c, the increase in fluctuations begins during the transition into stage IV, which also coincides with a rapid growth rate. Therefore, the beginning of consistent fluctuations in the first derivates values provides a good indication that the granules have reached their maximum pore saturation and have begun to form large agglomerates or clusters. The fluctuations remain present and increase as granulation continues beyond the end-point and enters the over-wetted stage. In Fig. 9, an arbitrary limit at $+/- 0.3$ was added to draw readers attention to the fluctuations. This limit could also be utilized as a control limit to signify a method of alarming users that granulation is approaching the end-point when both the upper and lower limit is consistently triggered, indicating high fluctuations. It is important to note that this limit is dependent on the frequency of recorded torque data, equipment type, processing conditions, and the desired product quality, and thus its implementation to different systems and experimental designs will require user discretion.

4. Summary

This work evaluated torque profiles obtained from granulation runs of different formulations and process conditions and categorized the profiles into two different types – type 1 and type 2. The obvious difference between the two curve types is that in the type 2 profile, the stage III plateau phase was not observed. Through the use of a classification tree, we identified the key input factors that distinguish the various torque profiles in our study. Specifically, the binder and API type were the most important factors, and impeller speed was also a contributing factor for ACM formulations. Finally, the end-point markers identified in the torque profiles based on a target size specification were at the beginning of the plateau phase for type 1 curves and on the transition between stages II and IV for type 2 curves. Nevertheless, it can be challenging to identify the end-points of the torque profile without a full picture of the trends. Thus, the fluctuations of the first derivative of the torque values were proposed as a method to monitor the granulation process and signify approaching targeted end-points.

Declaration of Competing Interest

None.

Data availability

Data will be made available on request.

Credit Author Statement.

Ashley Dan: Conceptualization, Methodology, Original draft preparation. **Haresh Vaswani:** Investigation. **Alice** Šimonová**:** Investigation. Aleksandra Grząbka-Zasadzińska: Investigation.

Jingzhe Li**:** Validation. Koyel Sen: Validation. Shubhajit Paul: Supervision. Yin-Chao Tseng: Supervision. Rohit Ramachandran: Supervision, Reviewing and Editing.

Declaration of interests

The authors declare the following financial interests/personal relationships which may be considered as potential competing interests:

Rohit Ramachandran reports equipment, drugs, or supplies was provided by Rutgers The State University of New Jersey.

References

Belem, B.R., Ferraz, H.G., 2020. Rheological profile in mixer torque rheometer of samples containing furazolidone and different binders. Chem. Eng. Res. Des. 160, 533–539.

Bier, H., 1979. Determination of the uncritical quantity of granulating liquid by power consumption measurement on planetary mixers. Pharm Ind. 41, 375–380.

Bouwman, A., Henstra, M., Hegge, J., Zhang, Z., Ingram, A., Seville, J., Frijlink, H., 2005. The relation between granule size, granule stickiness, and torque in the high-shear granulation process. Pharm. Res. 22, 270–275.

Cavinato, M., Andreato, E., Bresciani, M., Pignatone, I., Bellazzi, G., Franceschinis, E., Realdon, N., Canu, P., Santomaso, A.C., 2011. Combining formulation and process aspects for optimizing the high-shear wet granulation of common drugs. Int. J. Pharm. 416 (1), 229–241.

Cavinato, M., Bresciani, M., Machin, M., Bellazzi, G., Canu, P., Santomaso, A.C., 2010. Formulation design for optimal high-shear wet granulation using on-line torque measurements. Int. J. Pharm. 387 (1–2), 48–55.

Censi, R., Martena, V., Hoti, E., Malaj, L., Di Martino, P., 2013. Sodium ibuprofen dihydrate and anhydrous: study of the dehydration and hydration mechanisms. J. Therm. Anal. Calorim. 111, 2009–2018.

Han, S., Hong, J., Luo, Q., Xu, H., Tan, H., Wang, Q., Tao, J., Zhou, Y., Peng, L., He, Y., 2022. Hygroscopicity of organic compounds as a function of organic functionality, water solubility, molecular weight, and oxidation level. Atmos. Chem. Phys. 22 (6), 3985–4004.

Hansuld E, Briens L. 2014. A review of monitoring methods for pharmaceutical wet granulation. Int. J. Pharm. 472(1–2):192–201.

Holm, P., Schaefer, T., Kristensen, H., 1985a. Granulation in high-speed mixers Part V. Power consumption and temperature changes during granulation. Powder Technol. 43 (3), 213–223.

Holm, P., Schaefer, T., Kristensen, H., 1985b. Granulation in high-speed mixers Part VI. Effects of process conditions on power consumption and granule growth. Powder Technol. 43 (3), 225–233.

Iveson, S.M., Litster, J.D., 1998. Growth regime map for liquid-bound granules. AICHE J. 44 (7), 1510–1518.

Iveson, S.M., Litster, J.D., Hapgood, K., Ennis, B.J., 2001a. Nucleation, growth and breakage phenomena in agitated wet granulation processes: a review. Powder Technol. 117 (1–2), 3–39.

Iveson, S.M., Wauters, P.A., Forrest, S., Litster, J.D., Meesters, G.M., Scarlett, B., 2001b. Growth regime map for liquid-bound granules: further development and experimental validation. Powder Technol. 117 (1–2), 83–97.

Kašpar, O., Tokárová, V., Oka, S., Sowrirajan, K., Ramachandran, R., Štěpánek, F., 2013. Combined UV/Vis and micro-tomography investigation of acetaminophen dissolution from granules. Int. J. Pharm. 458 (2), 272–281.

Köster, C., Pohl, S., Kleinebudde, P., 2021. Evaluation of binders in twin-screw wet granulation. Pharmaceutics. 13 (2), 241.

Leuenberger, H., Bier, H., Sucker, H., 1981. Determination of the liquid requirement for a conventional granulation process. Ger Chem Eng. 4, 13–18.

Leuenberger, H., Puchkov, M., Krausbauer, E., Betz, G., 2009. Manufacturing pharmaceutical granules: is the granulation end-point a myth? Powder Technol. 189 (2), 141–148.

Lin, C.-Y., Wang, H.-C., Hsu, W.-Y., Huang, A.-N., Kuo, H.-P., 2019. Stage-wise characterization of the high shear granulation process by impeller torque changing rate. Adv. Powder Technol. 30 (8), 1513–1521.

Liu, B., Wang, J., Zeng, J., Zhao, L., Wang, Y., Feng, Y., Du, R., 2021. A review of high shear wet granulation for better process understanding, control and product development. Powder Technol. 381, 204–223.

Ly, A., Achouri, I.E., Gosselin, R., Abatzoglou, N., 2021. Wet granulation end point prediction using dimensionless numbers in a mixer torque rheometer: Relationship between capillary and Weber numbers and the optimal wet mass consistency. Int. J. Pharm. 605, 120823.

Mackaplow, M.B., Rosen, L.A., Michaels, J.N., 2000. Effect of primary particle size on granule growth and endpoint determination in high-shear wet granulation. Powder Technol. 108 (1), 32–45.

Meng, W., Kotamarthy, L., Panikar, S., Sen, M., Pradhan, S., Marc, M., Litster, J.D., Muzzio, F.J., Ramachandran, R., 2016. Statistical analysis and comparison of a continuous high shear granulator with a twin screw granulator: effect of process parameters on critical granule attributes and granulation mechanisms. Int. J. Pharm. 513 (1–2), 357–375.

Nagai, T., Prakongpan, S., 1984. Solubility of acetaminophen in cosolvents. Chem. Pharm. Bull. 32 (1), 340–343.

Oka, S., Kašpar, O., Tokárová, V., Sowrirajan, K., Wu, H., Khan, M., Muzzio, F., Štěpánek, F., Ramachandran, R., 2015. A quantitative study of the effect of process parameters on key granule characteristics in a high shear wet granulation process involving a two component pharmaceutical blend. Adv. Powder Technol. 26 (1), 315–322.

Otsu, T., Nakamura, H., Ohsaki, S., Watano, S., Fujiwara, S., Higuchi, T., 2022. Determining Optimum Water Content for Iron Ore Granulation using Agitation Torque of Wet Ore Powder. ISIJ Int. 62 (7), 1381–1388.

Paul, S., Sun, C.C., 2017. The suitability of common compressibility equations for characterizing plasticity of diverse powders. Int. J. Pharm. 532 (1), 124–130.

Rowe, R.C., Sheskey, P., Quinn, M., 2009. Handbook of Pharmaceutical Excipients. Libros Digitales-Pharmaceutical Press.

Ryckaert, A., Stauffer, F., Funke, A., Djuric, D., Vanhoorne, V., Vervaet, C., De Beer, T., 2021. Evaluation of torque as an in-process control for granule size during twin-screw wet granulation. Int. J. Pharm. 602, 120642.

Sampat, C., Kotamarthy, L., Bhalode, P., Chen, Y., Dan, A., Parvani, S., Dholakia, Z., Singh, R., Glasser, B.J., Ierapetritou, M., 2022. Enabling energy-efficient manufacturing of pharmaceutical solid oral dosage forms via integrated techno-economic analysis and advanced process modeling. Journal of Advanced Manufacturing and Processing. 4 (4), e10136.

Sakr, W.F., Ibrahim, M.A., Alanazi, F.K., Sakr, A.A., 2012. Upgrading wet granulation monitoring from hand squeeze test to mixing torque rheometry. Saudi Pharmaceutical Journal. 20 (1), 9–19.

Schweitzer, M., Pohl, M., Hanna-Brown, M., Nethercote, P., Borman, P., Hansen, G., Smith, K., Larew, J., 2010. Implications and opportunities of applying QbD principles to analytical measurements. Pharm. Technol. 34 (2), 52–59.

Simon, L.L., Pataki, H., Gr, Marosi, Meemken, F., Hungerbühler, K., Baiker, A., Tummala, S., Glennon, B., Kuentz, M., Steele, G., 2015. Assessment of recent process analytical technology (PAT) trends: a multiauthor review. Org. Process Res. Dev. 19 (1), 3–62.

Terashita, K., Watano, S., Miyanami, K., 1990. Determination of end-point by frequency analysis of power consumption in agitation granulation. Chem. Pharm. Bull. 38 (11), 3120–3123.

Thapa, P., Tripathi, J., Jeong, S.H., 2019. Recent trends and future perspective of pharmaceutical wet granulation for better process understanding and product development. Powder Technol. 344, 864–882.

US Food and Drug Administration. 2004. Guidance for industry, PAT-A framework for innovative pharmaceutical development, manufacturing and quality assurance. http ://wwwfda gov/cder/guidance/published html.

Food, U.S., Administration, Drug, 2009. Guidance for Industry, Q8 (R2) Pharmaceutical Development.

Walker, E.C., McGregor, N.E., Chan, A.S., Sims, N.A., 2021. Measuring bone volume at multiple densities by micro-computed tomography. Bio-protocol. 11 (1), e3873.

Yu, L.X., Amidon, G., Khan, M.A., Hoag, S.W., Polli, J., Raju, G., Woodcock, J., 2014. Understanding pharmaceutical quality by design. AAPS J. 16 (4), 771–783.

Yu, L.X., Kopcha, M., 2017. The future of pharmaceutical quality and the path to get there. Int. J. Pharm. 528 (1–2), 354–359.